A simple atmosphere-ocean model of tropical Atlantic decadal variability: Interaction between zonal and meridional modes

S.-K. Lee[1] and C. Wang[2]

[1] Cooperative Institute for Marine and Atmospheric Studies, University of Miami, Miami FL
[2] Atlantic Oceanographic and Meteorological Laboratory, NOAA, Miami FL

Submitted to Journal of Physical Oceanography
September 2005

Abstract. Simple atmosphere-ocean coupled models are used to study the interaction between the zonal and meridional modes of tropical Atlantic decadal variability. Perturbing the model tropical Atlantic only from the subtropics (25-30^{o}) with a decadal frequency, inter-hemispheric SST dipole mode emerges due to the Wind-Evaporation-SST feedback. Near the equator, the cross-equatorial oceanic gyre circulation develops due to the dipole-induced wind stress curl. This oceanic gyre transports surface water across the equator from the cold to the warm hemisphere in the western boundary and from the warm to the cold hemisphere in the Sverdrup interior. Interestingly, this happens during both positive and negative phases of the dipole oscillation, thus producing a persistent positive zonal SST gradient along the equator. Later, Bjerknes-type feedback kicks in, strengthening the zonal SST gradient. After one or two forcing cycles, this feature eventually grows to a stationary stage sustaining the uplift (depression) of the equatorial thermocline in the west (east), and equatorial westerly wind anomalies, a condition similar to Atlantic-Niño. Further modeling results are presented to argue that the coupled model has some skills in reproducing the observed low-frequency fluctuation of the tropical Atlantic SST, thus a significant portion of tropical Atlantic decadal variability is remotely forced from the subtropics.

1. Introduction

Unlike the tropical Pacific, climatic fluctuations over the tropical Atlantic are largely forced by perturbations of remote origins, such as El Niño-Southern Oscillation (ENSO) and North Atlantic Oscillation (NAO) (Curtis and Hastenrath, 1995; Nobre and Shukla, 1996; Enfield and Mayer, 1997; Czaja et al. 2002; Enfield et al. 2006). Tropical Atlantic variability (TAV) includes two major modes, namely the Atlantic-Niño and dipole modes (a preferable terminology for the latter is cross-equatorial SST gradient mode, or simply meridional mode, but here we use these terms interchangeably). The first mode is analogous to ENSO in the Pacific and prevails at the interannual time scale, but requires external perturbations to sustain finite-amplitude oscillations (Zebiak, 1993). The second mode, on the other hand, is dominant at the decadal time scale and the associated sea surface temperature anomaly is most pronounced off the equator around 10-15^{o} latitude band (Chang et al., 1997; Xie, 1999). Like the Atlantic-Niño mode, the meridional mode is weakly damped (*i.e*, not self-sustainable) (Xie, 1999), thus anti-symmetric configurations of sea surface temperature anomaly are not ubiquitous in the tropical Atlantic (Enfield et al. 1999). Nevertheless, using a semi-empirical model for the relationship between surface heat flux and SST, Chang et al. (1997) find that the interactions of the ocean and atmosphere through surface heat flux give rise to decadal oscillations of dipole structure similar to observations (*e.g*., Nobre and Shukla, 1996). Consistent with this finding, Xie (1999) demonstrated clearly that a dipole sea surface temperature pattern could emerge in a simple atmosphere-ocean coupled model of the tropical Atlantic through the Wind-Evaporation-SST (WES) feedback (Xie and Philander, 1994) if the decadal forcing from subtropics is robust enough. Recently, Okajima et al. (2003) show that this is more likely to occur if the ITCZ is close to the equator, as it is in boreal spring, and that the tendency to form a dipole is suppressed

when the ITCZ is off the equator suggesting a seasonal phase locking mechanism. Collectively, these studies suggest that the Atlantic dipole mode is not self-sustaining, thus it is critically dependent upon the mid-latitude forcing patterns, but even in the absence of inter-hemispheric SST anti-correlation, significant (more than 95% confidence limit) cross-equatorial SST gradients occur frequently (about 50% of the time during 1856-1991 according to Enfield et al. 1999) and can be associated with climate variability in the tropical Atlantic region (Wang, 2002). Indeed, a recent Coupled General Circulation Model (CGCM) study by Huang and Shukla (2005) shows that the WES feedback can prevail in non-dipole configurations, causing midlatitudinal disturbances to propagate equatorward, in agreement with idealized model studies (Liu, 1996; Xie, 1997). See Xie and Carton (2004) for a complete review on patterns, mechanisms and impacts of TAV.

It has been suggested that tropical ocean dynamics do not have a major impact on TAV (Carton et al. 1996; Seager et al. 2001; Alexander and Scott, 2002; Chang et al., 2003; Barreiro et al. 2005; Saravanan and Chang, 2004; Joyce et al. 2004). However, some studies argue that the equatorial Atlantic Ocean dynamics are actively involved in TAV (*e.g.*, Servain et al., 1999; 2000). Using historical subsurface data obtained from XBT (expendable bathythermograph) drops, Servain et al. (1999) report that a significant correlation exists between the two tropical Atlantic modes at both decadal and interannual (1-2 years) time scales during 1979-93, and that both modes involve latitudinal displacements of the ITCZ as in the annual response. By confirming this through an Ocean General Circulation Model (OGCM) simulation, Servain et al. (2000) further propose that equatorial ocean dynamics may be the principal cause of tropical Atlantic climate variability. Murtugudde et al. (2001) present a partially supportive modeling result but adding that, although the two modes are significantly correlated for limited record

lengths prior to and after 1976, the correlation fall apart when longer time-series from 1949 to 2000 are considered due to the large shift in equatorial thermocline depth that occurred in late 1970s.

The focus of this study is to investigate whether tropical ocean dynamics play an active role in tropical Atlantic decadal variability. By using simple coupled models, we show that, in the decadal time scale, an Atlantic-Niño-like condition can be provoked by the dipole mode, thus supporting the hypothesis that the two climate modes (the Atlantic-Niño and meridional modes) are correlated in the decadal time scale. The atmosphere-ocean dynamics involved are, however, different from those suggested by Servain et al. (1999) because, in our case, the cross-equatorial oceanic gyre circulation plays a critical role. The framework for our modeling study closely follows Xie (1999). Here, we revise and extend his model by (1) allowing zonal variations in both atmosphere and ocean, and (2) replacing the slab ocean model with a fully dynamic 2.5 layer reduced gravity ocean model previously used in Lee and Csanady (1999b).

2. Models

The original Gill (1980) model is used for the atmosphere. The governing equations are written as (unless specified otherwise, all variables are perturbations from their mean states)

$$\varepsilon U - fV = -\frac{\partial P}{\partial x}, \tag{2.1}$$

$$\varepsilon V + fU = -\frac{\partial P}{\partial y}, \tag{2.2}$$

$$\varepsilon P + C^2\left(\frac{\partial U}{\partial x} + \frac{\partial V}{\partial y}\right) = -KT_1, \tag{2.3}$$

where U and V are the zonal and meridional components of surface wind perturbation, P is the surface pressure anomaly, T_1 the sea surface temperature anomaly, f the Corioles parameter, C the internal gravity wave speed, ε the damping rate, and K the thermal coupling coefficient.

The ocean model is a 2.5 layer reduced gravity model (Lee and Csanady, 1999b; Schopf and Cane, 1983) consisting of two active layers, the surface mixed layer and the thermocline layer, on top of the stagnant deep layer. The momentum and continuity equations, linearized from the mean state, can be written as

$$\frac{\partial \mathbf{v}_1}{\partial t} - f\mathbf{k} \times \mathbf{v}_1 = \frac{1}{\rho_0}\nabla p_1 + \frac{c_d \mathbf{V}}{\rho_0 H_1} + A_h \nabla^2 \cdot \mathbf{v}_1 , \tag{2.4}$$

$$\frac{\partial \mathbf{v}_2}{\partial t} - f\mathbf{k} \times \mathbf{v}_2 = \frac{1}{\rho_0}\nabla p_2 + A_h \nabla^2 \cdot \mathbf{v}_2 , \tag{2.5}$$

$$\frac{\partial h_1}{\partial t} + H_1 \nabla \cdot \mathbf{v}_1 = w_e , \tag{2.6}$$

$$\frac{\partial h_2}{\partial t} + H_2 \nabla \cdot \mathbf{v}_2 = -w_e , \tag{2.7}$$

where $\mathbf{v}_1$ and $\mathbf{v}_2$ are the velocity anomaly vectors for the two active layers, h_1 and h_2 are the thickness perturbations from their mean values H_1 and H_2, c_d is the drag coefficient, A_h the horizontal momentum diffusion coefficient. On the basis of the hydrostatic relation, the pressure gradient terms are given by

$$\nabla p_1 = g\alpha\nabla\left[h_1\left(\overline{T}_1 - \overline{T}_3\right) + h_2\left(\overline{T}_2 - \overline{T}_3\right)\right] - \tfrac{1}{2} g\alpha H_1 \nabla T_1 , \tag{2.8}$$

$$\nabla p_2 = g\alpha\nabla\left[\left(h_1 + h_2\right)\left(\overline{T}_2 - \overline{T}_3\right)\right], \tag{2.9}$$

where α is the thermal expansion coefficient, $\overline{T}_1$, $\overline{T}_2$ and $\overline{T}_3$ are mean state temperature of the two active layers and the deep inert layer, respectively. The entrainment/detrainment rate, w_e, is parameterized as linearly dependent on the mixed layer depth anomaly, h_1:

$$w_e = -\gamma h_1 , \tag{2.10}$$

where the vertical mixing coefficient γ is set to $(365\text{day})^{-1}$.

The thermodynamic equation for the mixed layer can be written as

$$\begin{aligned} \frac{\partial T_1}{\partial t} + \left(\overline{\mathbf{v}}_\mathbf{1} \cdot \nabla T_1 + \mathbf{v}_\mathbf{1} \cdot \nabla \overline{T}_1 + \mathbf{v}_\mathbf{1} \cdot \nabla T_1\right) = & \frac{\overline{Q}_e}{c_p \rho_0 H_1}\left[\frac{\overline{U}U + \overline{V}V}{\overline{U}^2 + \overline{V}^2}\right] - rT_1 \\ & - \frac{w_e}{H_1}\left(\overline{T}_1 - \overline{T}_2\right) + A_T \nabla^2 T_1 + F, \end{aligned} \tag{2.11}$$

where the overbar denotes the mean state variable, c_p is the specific heat of water, r the thermal damping coefficient, A_T the thermal diffusion coefficient, $\overline{Q}_e$ the latent heat flux of the mean state (positive downward), $\overline{U}$ and $\overline{V}$ are the zonal and meridional wind component of the mean state, respectively, and F is the external forcing to be described later. Note that the temperatures of the lower layers remain constant (*i.e.*, $T_2 = T_3 = 0$). The first term on the rhs of (2.11) is obtained by linearizing the bulk formula for latent heat flux (see Liu, 1996 and Xie, 1999 for detailed derivation) and it is the central component for the WES feedback to occur in the coupled model. The second term on the rhs is the thermal damping term arising from temperature dependence of latent heat flux, and the third is the entrainment/detrainment term that is particularly important for the Atlantic zonal mode. The three terms inside the bracket on the lhs of (2.11) are advective heat flux divergence terms. It is assumed that the mean state is motionless and has constant mixed layer temperature, thus the first two terms vanish and only remaining term is the nonlinear one. It will be shown in the following section that this nonlinear advection term plays the key role in the interaction of the two Atlantic climate modes in the decadal time scale.

The model Atlantic domain is a rectangular box, extending zonally from 80°W to 20°E and meridionally from 30°S to 30°N, with the model resolution of roughly 0.7°. The north and south

boundaries are closed with a slip-condition applied at all sidewalls. The mean ocean state is 200m deep (h_1=100m; h_2=100m) with the thermal parameters chosen to yield two internal gravity wave speeds of 2.5 and 1.0 ms^{-1}. All model parameters and their values used in this study are listed in Table 1. These values in the table are chosen to be identical to those used in Xie (1999) except for three coupling parameters, namely the thermal coupling coefficient, *K,* the thermal damping coefficient, *r* and the drag coefficient c_d. These values are appropriately chosen to ensure that the simulated WES feedback is weakly damped in the tropical Atlantic model configuration with the intrinsic resonant period at approximately 10 years, as indicated in previous observational and modeling studies. For comparison with our dynamically coupled model runs (Gill-reduced gravity ocean model or simply Gill-rgom hereafter), the Gill atmospheric model is also coupled to a slab ocean model (Gill-slab hereafter). The slab thermodynamic equation can be thus written as

$$\frac{\partial T_1}{\partial t} = \frac{\overline{Q}_e}{c_p \rho_0 H_1}\left[\frac{\overline{U}U + \overline{V}V}{\overline{U}^2 + \overline{V}^2}\right] - rT_1 + A_T \nabla^2 T_1 + F\,. \tag{2.12}$$

In all model runs, in order to mimic the decadal midlatitude perturbations typically caused by NAO (25-30^{o}N lies on the border between the middle and southern parts of the SST tripole associated with the NAO according to Marshall et al. 2001), sea surface temperature perturbations are imposed only between 25^o and 30^o (in both hemispheres) with the forcing period of 10 years. Coupled model runs are carried out using an anti-symmetric midlatitude forcing patterns, *i.e.*, the sign of forcing is opposite in the two hemispheres but with the same amplitude, thus the forcing term *F* in (2.11) and (2.12) is given by

$$c_p \rho_0 H_1 F = \begin{cases} \kappa \cdot \cos\left(2\pi/10\,\mathrm{yr} \cdot t\right) & \text{for } y = 25^o\mathrm{N} - 30^o\mathrm{N} \\ 0 & \text{for } y = 25^o\mathrm{S} - 25^o\mathrm{N} \\ -\kappa \cdot \cos\left(2\pi/10\mathrm{yr} \cdot t\right) & \text{for } y = 25^o\mathrm{S} - 30^o\mathrm{S}, \end{cases} \tag{2.13}$$

where κ is set to $(365\text{day})^{-1}$. In the following section, the two coupled model runs (Gill-slab and Gill-rgom) under this forcing (2.13) are used to describe the atmosphere-ocean feedback dynamics. The model results are then compared with observations and also with a Hybrid Coordinate Ocean Circulation Model (HYCOM) run forced with the ECMWF 40-year global reanalysis (Brankovic and Molteni, 2004) surface heat flux data (More details about this HYCOM simulation can be found in Lee et al. 2005).

3. Results

Fig. 1a shows the latitude-time structure of the zonally averaged sea surface temperature anomaly and wind anomaly components simulated by the Gill-slab model under the anti-symmetric midlatitude forcing. The structure of the solution closely resembles the WES feedback mode studied earlier by Xie (1999), showing clearly the SST see-saw pattern north and south of the equator that slowly propagates equatorward, and the cross-equatorial winds blowing from the cold to the warm hemisphere. As explained by Liu (1996), the equatorial propagation can be understood as follows. A warm SST anomaly in the tropics produces a westerly wind anomaly on the equator side and an easterly wind anomaly on the poleward side. The westerly wind anomaly reduces the mean trade wind while the easterly wind anomaly increases the mean wind. The associated latent heat flux produces warming on the equator side and cooling on the poleward side, thus causing the warm SST anomaly to propagate toward the equator.

Fig. 1b is the same as Fig. 1a but for the Gill-rgom run. The most striking difference between the two cases is that the amplitude of anomalous signal is much weaker when ocean dynamics are activated in the coupling process (Fig. 1b), suggesting that local ocean dynamics contribute to the damping of Atlantic dipole mode in agreement with earlier studies (*e.g.*, Carton et al.

1996; Seager et al. 2001; Joyce et al. 2004). The most likely mechanisms for the damping are the inter-hemispheric heat exchange due to ocean dynamics (Joyce et al. 2004), and the Ekman-upwelling (downwelling) in the warm (cold) hemisphere. However, it appears that ocean dynamics do more than just damping because the latitude-time structure of the solution is also altered. In particular, the location of the nodal point (zero contour lines of SST anomalies) is shifted about 2-3^{o} off the equator toward the cold hemisphere, and the center of the maximum amplitude meridional wind anomalies is also shifted accordingly, displaying a meandering pattern in latitude-time space.

Fig. 2a and 2b show model solutions (sea surface temperature and wind anomalies) for the Gill-slab and the Gill-rgom cases, respectively. Shown in the upper panel is the average for the model year 22, 23 and 24 (a positive phase: warm in the north and cold in the south), and the lower panel for the model year 27, 28 and 29 (a negative phase: cold in the north and warm in the south). The structure of the oscillating solution shown in Fig 2a is very similar to the zonally uniform solution of Xie (1999), but anomalous SST and winds are more pronounced toward the west. This feature appears to originate from westward propagating WES waves that amplify as they move westward (Xie, 1996). The difference between the two cases (Gill-slab and Gill-rgom) is quite substantial especially within the equatorial band where zonally uniform SST structure in the Gill-slab run is nearly collapsed in the Gill-rgom run. A positive zonal SST gradient (increase eastward) persists in the equator during both positive and negative phases of the dipole oscillation. Relatively weak but persistent westerly anomalies prevail along the central and eastern sides of the equator reinforcing the positive zonal SST gradient there, suggestive of a Bjerknes-type positive feedback.

Fig. 3a displays oceanic mixed layer depth (h_1) and transport (u_1H_1 and v_1H_1) anomalies corresponding to the sea surface temperature and wind perturbation shown in Fig 2b. A close inspection of Fig. 3a along with Fig. 2b suggests that the cross-equatorial oceanic gyre circulation emerges due to the wind stress curl pattern associated with the inter-hemispheric SST dipole (Joyce et al. 2004). This gyre circulation allows a cross-equatorial transport of the mixed layer water from the cold to the warm hemisphere in the western boundary and from the warm to cold hemisphere in the Sverdrup interior. Interestingly, this happens during both positive and negative phases of the dipole oscillation, thus a negative (positive) SST anomaly persists in the western (central and eastern) equatorial Atlantic (see Fig 2b). In turn, this equatorial SST anomaly drives westerly wind anomalies, thereby uplifting (depressing) the equatorial thermocline in the west (east). Anomalous cooling (warming) by entrainment (detrainment) in the west (east) allows the equatorial SST and wind anomalies to grow stronger (not shown), closing a positive atmosphere-ocean feedback loop. Fig. 3b shows the depth of thermocline layer (h_1+h_2) and transport (u_2H_2 and v_2H_2) anomalies. Oscillations of the thermocline depth and associated transport anomalies off the equator are similar to those simulated by using 1.5 layer ocean model forced with a dipole-induced wind stress pattern (Joyce, 2004). Near the equator, however, the westward equatorial undercurrent anomalies persist during both positive and negative phases of the dipole oscillation due to the pressure gradient anomaly along the equator.

In summary, the cross-equatorial oceanic gyre circulation appears to be directly responsible for inducing the positive zonal SST gradient along the equator but subsequent atmosphere-ocean positive feedback further intensifies the zonal SST gradient, eventually creating a condition similar to Atlantic-Niño. The longitude-time structure of the equatorial mixed layer depth (not shown) reveals that one or two forcing cycles are required for the zonal pattern to grow to a fully

mature stage, Once it reaches its full strength, however, the zonal structure becomes nearly stationary feeding its energy from the WES feedback that in turn requires decadal perturbations from midlatitude.

In order to test if our conclusion can be verified, we carry out another model experiment. The same Gill-rgom is forced from the midlatitude (25 – 30^{o}), but this time, with the observed zonally-averaged sea surface temperature anomaly (Smith and Reynolds, 2004) instead of the anti-symmetric forcing. Fig. 4 shows the latitude-time evolution of the (a) simulated versus (b) observed (three-year running mean) sea surface temperature anomaly between 20^{o}S and 20^{o}N. Although there are many noticeable differences between the model result and the observation, the model seems to capture some low-frequency fluctuations of the observed sea surface temperature anomaly. In particular, the model shows a positive dipole phase before mid-1970s, followed by a negative phase between mid-1975s and mid-1990s. This feature is consistent with the shift in NAO that occurred around mid-1970s from a negative to a positive phase (Hurrell, 1995), thus it seems to present in the observation too, although in the observation it is masked by much complicated oscillation patterns that are in many cases in non-dipole structure. The similarity between the modeled and observed SST patterns suggests that a significant portion of tropical Atlantic decadal variability is remotely forced from the midlatitudes.

Shown in Fig. 5 is the longitude-time structure of (a) the simulated equatorial mixed layer depth, and (b) the 20^{o}C isotherm in the equatorial Atlantic (three-year running mean) obtained from a Hybrid Coordinate Ocean Circulation Model (HYCOM) run forced with the ECMWF 40-year global reanalysis (Brankovic and Molteni, 2004) surface heat flux data (see Lee et al. 2005 for more details about the HYCOM simulation). Again, there are large differences between the coupled model result and the HYCOM simulation. It is noted that there is a large shift in the

zonal slope of the equatorial thermocline around mid-1970s in the HYCOM simulation, from a weak to a strong phase, in agreement with the earlier OGCM study of Murtugudde et al. (2001). The coupled model also shows a similar shift, but it takes place much later in mid-1980s, thus it is not conclusive whether this shift in the equatorial thermocline is subject to the same dynamics as in the OGCM simulation.

4. Summary and Discussions

Simple coupled models are used to investigate how ocean dynamics interact with the atmosphere in tropical Atlantic decadal variability. Our model results suggest that ocean dynamics play an important role by inducing a zonal structure in tropical Atlantic decadal variability that is otherwise largely sustained by the meridional SST gradient mode. Forced by the dipole-induced wind stress curl, the cross-equatorial oceanic gyre circulation develops near the equator. This ocean gyre transports equatorial surface water from the cold to the warm hemisphere in the western boundary and from the warm to the cold hemisphere in the Sverdrup interior. Since this happens during both positive and negative phases of the dipole oscillation, a positive zonal SST gradient persists along the equator. Later, Bjernes-type positive feedback kicks in, thus the zonal SST gradient grows stronger. The final outcome is the uplift (depression) of the equatorial thermocline in the west (east), and equatorial westerly wind anomalies, a condition similar to Atlantic-Niño. Figure 6 shows a sketch of this interaction mechanism between zonal and meridional modes.

Although not shown here, additional experiments are performed with different midlatitude forcing patterns. From those experiments, we find that the WES feedback mechanism still works under a symmetric midlatitude forcing pattern with and without ocean dynamics, but the

oscillations are much weaker. Interestingly, the stationary Atlantic-Niño-like feature that prevails under the anti-symmetric midlatitude forcing does not exist in this case. On the other hand, if the midlatitude forcing is confined in the northern or southern hemisphere only, the stationary Atlantic-Niño-like condition does develop but with much reduced growth rate. These results collectively suggest that inter-hemispheric SST contrast is the precondition for generating the stationary Atlantic-Niño-like condition. It is also important to note that the decadal perturbation from the midlatitude is the ultimate source of the oscillations, because the meridional mode has the intrinsic resonant period at the decadal timescale and is not self-sustainable. Hence, the stationary Atlantic-Niño-like pattern is not evoked without the inter-hemispheric SST contrast, and it cannot be excited at the interannual timescale.

It is a difficult task to confirm our finding that the strengthening of inter-hemispheric SST gradient mode contributes to Atlantic-Niño-like conditions, particularly due to the complexity of the tropical Atlantic system where both remotely forced and internally generated signals are all mixed together. We also recognize the limitations of our coupled model (Gill-rgom) involved in neglecting the mean flow effect and also the teleconnection from the equatorial Pacific via the anomalous Walker circulation (Latif and Grotzner, 2000). An important question is whether the suggested dynamic relationship between the meridional and zonal modes is robust enough to stand out as important tropical Atlantic climate variability. To answer this question, we need to further investigate using more realistic models. In particular, we need to consider the seasonal mean flow effect in equation (2.11) and also to use more complex scheme for the turbulent mixing parameterization (2.10). We are currently working to improve our coupled model in these respects, and to test our hypothesis using a fully coupled general circulation model. It is expected that these improvements in the coupled model bring significant changes in the model behavior.

For instance, it is conceivable that the meridional exchanges of heat and mass through the Atlantic subtropical cells dominate tropical Atlantic decadal variability (Larzar et al., 2001). However, we also want to argue that our coupled model without these improvements still demonstrates some skills in reproducing the low-frequency fluctuations of the observed sea surface temperature, and also the depth of the equatorial thermocline to a certain extent. This suggests that a significant portion of tropical Atlantic decadal variability is remotely forced from the midlatitudes, and that the equatorial thermocline can be affected by the meridional mode in the decadal time scale. Moreover, since the equatorial Atlantic ocean serves as the important gateway of the inter-hemispheric mass and heat transport (e.g., Lee and Csanady, 1999a), the decal shift in the equatorial thermocline contribute to the weakening of the equatorial Atlantic circulation system, thus to the shifting of climate in the region, and possibly to the fluctuation of the Atlantic thermohaline circulation.

Acknowledgements. This research was supported by the NOAA PACS/GAPP Program through awards under Cooperative Agreement NA67RJO149 to the Cooperative Institute for Marine and Atmospheric Studies. We are indebted to D. Enfield for many scientific discussions and encouragement. Comments from D. Enfield, A. Mestas-Nuñez and R. Molinari help improve the manuscript. The findings and conclusions in this report are those of the authors and do not necessarily represent the views of the funding agency.

References

Alexander, M., and J. Scott, 2002: The influence of ENSO on air-sea interaction Atlantic, Geophys. Res. Lett.. 29, doi: 10.1029/2001GL014347.

Barreiro, M., P. Chang, L. Ji, R. Saravanan and A. Giannini, 2005: Dynamical elements of predicting boreal spring tropical Atlantic sea-surface temperatures, Dyn. Atmos. Oceans, 39, 61-85.

Brankovic, C. and F. Molteni, 2004: Seasonal climate and variability of the ECMWF ERA-40 model. Climate Dyn., *22*, 139-155.

Carton, J. A., X. H. Cao, B. S. Giese, and A. M. da Silva, 1996: Decadal and interannual SST variability in the tropical Atlantic Ocean. J. Phys. Oceanogr., 26, 1165-1175.

Chang, P., L. Ji, and H. Li, 1997: A decadal climate variation in the tropical Atlantic Ocean from thermodynamic air-sea interactions. Nature, 385, 516-518.

Chang, P., L. Ji, and R. Saravanan, 2001: A hybrid coupled model study of tropical Atlantic variability. J. Clim., 14, 361-390.

Chang, P., R. Saravanan, and L. Ji, 2003: Tropical Atlantic Seasonal Predictability: the Roles of El Niño remote influence and thermodynamic air-sea feedback. Geophys. Res. Lett., 30, 1501-1504.

Curtis, S. and S. Hastenrath, 1995: Forcing of anomalous sea surface temperature evolution in the tropical Atlantic during Pacific warm events. J. Geophys. Res., 100, 15835-15847.

Czaja, A., P. Van der Vaart, and J. Marshall, 2002: A diagnostic study of the role of remote forcing in tropical Atlantic variability. J. Clim., 15, 3280-3290.

Enfield, D. B. and D. A. Mayer, 1997: Tropical Atlantic sea surface temperature variability and its relation to El Niño-Southern Oscillation. J. Geophys. Res., 102, 929-945.

Enfield, D. B., A. M. Mestas-Nuñez, D. A. Mayer, and L. Cid-Serrano, 1999: How ubiquitous is the dipole relationship in tropical Atlantic sea surface temperatures? J. Geophys. Res., 104, 7841-7848.

Enfield, D. B., S.-K. Lee, and C. Wang, 2006: How are large Western Hemisphere Warm Pools formed? Progress in Oceangr., (in press).

Gill, A. E., 1980: Some simple solutions for heat-induced tropical circulation. Quart. J. Roy. Meteor. Soc., 106, 447–462.

Hurrell, J. W., 1995: Decadal trends in the North Atlantic Oscillation: Regional temperatures and precipitation, Science, 269, 676-679.

Huang, B. and J. Shukla. 2005: Ocean-Atmosphere Interactions in the Tropical and Subtropical Atlantic Ocean. J. Climate 18, 1652-1672.

Joyce, T. M., C. Frankignoul, J. Yang, H.E. Phillips, 2004: Ocean response and feedback to the SST dipole in the Tropical Atlantic. J. Phys. Oceanogr., 34, 2525-2540

Latif, M., and A. Grotzner, 2000: The equatorial Atlantic oscillation and its response to ENSO. Climate Dyn., 16, 213-218.

Lazar, A., R. Murtugudde, A. J. Busalacchi, A model study of temperature anomaly propagation from the subtropics to tropics within the South Atlantic thermocline, Geophys. Res. Lett., 28(7), 1271-1274, 10.1029/2000GL011418, 2001.

Lee, S.-K., G. T. Csanady, 1999a. Warm water formation and escape in the upper tropical Atlantic Ocean: 1. Literature review, J. Geophys. Res., 104, 29,561 – 29,571.

Lee, S.-K., G. T. Csanady, 1999b. Warm water formation and escape in the upper tropical Atlantic Ocean: 2. A numerical model study, J. Geophys. Res., 104, 29,573 – 29,590.

Lee, S.-K., D. B. Enfield, and C. Wang, 2005: Ocean general circulation model sensitivity experiments on the annual cycle of Western Hemisphere Warm Pool, J. Geophys. Res., 110, C09004, doi:10.1029/2004JC002640

Liu, Z. 1996: Modeling Equatorial Annual Cycle with a Linear Coupled Model. J. Clim., 9, 2376-2385.

Marshall, J., H. Johnson, and J. Goodman. 2001: A study of the interaction of the North Atlantic Oscillation with ocean circulation. J. Clim.,14, 1399–1421.

Murtugudde, R. G., J. Ballabrera-Poy, J. Beauchamp, A. J. Busalacchi, Relationship between zonal and meridional modes in the tropical Atlantic, Geophys. Res. Lett., 28(23), 4463-4466, 10.1029/2001GL013407, 2001.

Nobre, P. and J. Shukla, 1996: Variations of sea surface temperature, wind stress and rainfall over the tropical Atlantic and South America. J. Clim., 9, 2464-2479.

Okajima, H., S.-P. Xie, and A. Numaguti, 2003: Interhemispheric coherence of tropical climate variability: Effect of climatological ITCZ, J. Meteorol. Soc. Jpn., 81, 1371-1386.

Saravanan, R. and P. Chang, 2004: Thermodynamic coupling and predictability of tropical sea surface temperature, In Earth Climate: The Ocean-Atmosphere Interaction, C. Wang, S.-P. Xie and J.A. Carton (eds.), Geophys. Monogr., 147, AGU, Washington D.C., 171-180.

Schopf, P. S. and M. A. Cane, 1983: On Equatorial Dynamics, Mixed Layer Physics and Sea-Surface Temperature. J. Phys. Oceanogr., 13, 917-935.

Seager, R., Y. Kushnir, P. Chang, N. Naik, J. Miller and W. Hazeleger, 2001. Looking for the role of the ocean in tropical Atlantic decadal climate variability, J. Clim., 14, 638-655.

Servain, J. Jr., A. Dessier, Relationship between the equatorial and meridional modes of climatic variability in the tropical Atlantic, Geophys. Res. Lett., 26(4), 485-488, 10.1029/1999GL900014, 1999.

Servain, J. Jr., I. Wainer, H. L. Ayina, and H. Roquet, 2000. The relationship between the simulated climatic variability modes of the tropical Atlantic, Internat. J. Clim,. 20, 939 – 953.

Smith, T.M., and R.W. Reynolds, 2004: Improved Extended Reconstruction of SST (1854-1997). J. Clim., 17, 2466-2477.

Wang, C., 2002. Atlantic climate variability and its associated atmospheric circulation cells, J. Clim., 15, 1516 – 1536.

Xie, S.-P., and S.G.H. Philander, 1994: A coupled ocean-atmosphere model of relevance to the ITCZ in the eastern Pacific, Tellus, 46A, 340-350.

Xie, S.-P., 1996: Westward propagation of latitudinal asymmetry in a coupled ocean-atmosphere model. J. Atmos. Sci., 53, 3236-3250.

Xie, S.-P., 1997: Unstable Transition of the Tropical Climate to an Equatorially Asymmetric State in a Coupled Ocean-Atmosphere Model. Mon. Wea. Rev., 125, 667-679.

Xie, S.-P., 1999: A dynamic ocean-atmosphere model of the tropical Atlantic decadal variability. J. Clim., 12, 64-70.

Xie, S.-P. and J. A. Carton, 2004: Tropical Atlantic variability: Patterns, mechanisms, and impacts. Earth Climate: The Ocean-Atmosphere Interaction, C. Wang, S.-P. Xie and J.A. Carton (eds.), Geophys. Monogr., 147, AGU, Washington D.C., 121-141.

Zebiak, S. E., 1993. Air-sea interaction in the equatorial Atlantic region, J. Clim., 6, 1567 – 1586.

Table 1. Model parameters and their values used for model integrations. ATM indicates parameters used for the atmospheric model, OCN for the ocean model and CPL for the atmosphere-ocean coupling, respectively.

Parameter	Notation	Value
ε^{-1}	inverse of damping rate (ATM)	2 days
K	thermal coupling coefficient (ATM)	5.0×10^{-3} m^2 s^{-3} K^{-1}
C	internal gravity wave speed (ATM)	45 m s^{-1}
$\overline{U}$	zonal wind speed of the mean state (ATM)	-4.5 m s^{-1}
$\overline{V}$	meridional wind speed of the mean state (ATM)	0 m s^{-1}
A_h	Laplacian mixing coefficient for momentum (OCN)	2000 m^2 s^{-1}
ρ_0	density of sea water (OCN)	1020 kg s^{-1}
c_p	specific heat of water (OCN)	4200 m s^{-2} K^{-1}
α	thermal expansion coefficient (OCN)	2.5×10^{-4} K^{-1}
γ^{-1}	inverse of vertical mixing coefficient (OCN)	1 year
H_1	thickness of the mixed layer (OCN)	100 m
H_2	thickness of the thermocline layer (OCN)	100 m
$\overline{T}_1$	mean state temperature of the mixed layer (OCN)	25^{o}C
$\overline{T}_2$	mean state temperature of the thermocline layer (OCN)	20^{o}C
$\overline{T}_3$	mean state temperature of the deep motionless layer (OCN)	15^{o}C
$\overline{Q}_e$	latent heat flux of the mean state (positive downward) (CPL)	-125 W m^{-2}
r^{-1}	inverse of thermal damping coefficient (CPL)	0.5 year
c_d	drag coefficient (CPL)	2×10^{-2} N s m^{-3}
A_T	Laplacian mixing coefficient for heat (CPL)	2000 m^2 s^{-1}
κ	midlatitude forcing coefficient (CPL)	1 year

Figure captions

Figure 1. Latitude-time structure of the zonally averaged sea surface temperature anomaly (top panel) and wind anomaly components (zonal wind in the middle and meridional wind in the bottom), simulated by (a) the Gill-slab model and (b) the Gill-rgom model under the anti-symmetric mid-latitude forcing. The unit is ^{o}C for the sea surface temperature and ms^{-1} for the wind components. The contour interval is 0.5 for the sea surface temperature, 0.2 for the zonal wind and 0.1 for the meridional wind.

Figure 2. Sea surface temperature and wind anomalies simulated by (a) the Gill-slab model and (b) the Gill-rgom model. Shown in the upper panel is the average for the model year 22, 23 and 24 (positive phase: warm in the north and cold in the south), and the lower panel for the model year 27, 28 and 29 (negative phase: cold in the north and warm in the south). The maximum arrow is about 1.3 ms^{-1} for (a) and 0.7 ms^{-1} for (b). The contour interval is 0.2^{o}C.

Figure 3. Layer thickness and transport anomalies in the (a) mixed layer and (b) thermocline layer corresponding to the sea surface temperature and wind perturbation shown in Fig 2b. The maximum arrow is about 8.5 m^2s^{-1} for (a) and 4.5m^2s^{-1} for (b). The contour interval is 5m.

Figure 4. Latitude-time evolution of the (a) simulated versus (b) observed sea surface temperature anomaly (Smith and Reynolds, 2004), both averaged between 80^{o}W and 20^{o}E. The observed sea surface temperature anomaly is the three-year running mean.

Figure 5. Longitude-time structure of (a) the simulated equatorial mixed layer depth, and (b) the 20^{o}C isotherm in the equatorial Atlantic obtained from a HYCOM run forced with the ECMWF 40-year global reanalysis surface heat flux data (Lee et al. 2005). In both cases, the depth anomalies are averaged between 5^{o}S and 5^{o}N. The HYCOM output is the three-year running mean.

Figure 6. Sketch of the interaction mechanism between zonal and meridional modes during (a) positive and (b) negative phases of the dipole oscillation. Thicker arrows indicate wind perturbations. Dark shades are used for warm SST anomalies and light shades for cold SST anomalies. Closed circuits represent cross-equatorial gyre circulations that carry the tropical surface water toward the equator. Note that these gyre circulations supply cold water in the west and warm water in the Sverdrup interior during the both phases of dipole oscillation, producing a permanent Atlantic-Niño-like condition along the equator.

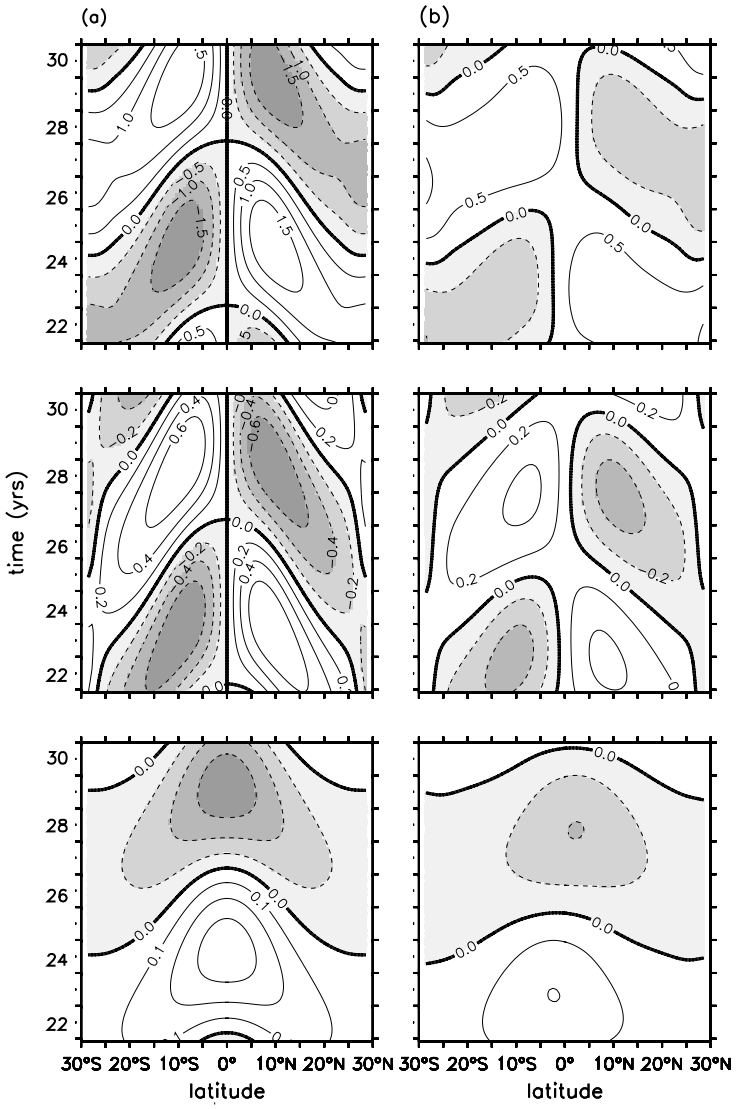
(a)
(b)
time (yrs)
30
28
26
24
22
30°S 20°S 10°S 0° 10°N 20°N 30°N
latitude
30°S 20°S 10°S 0° 10°N 20°N 30°N
latitude

Figure 1

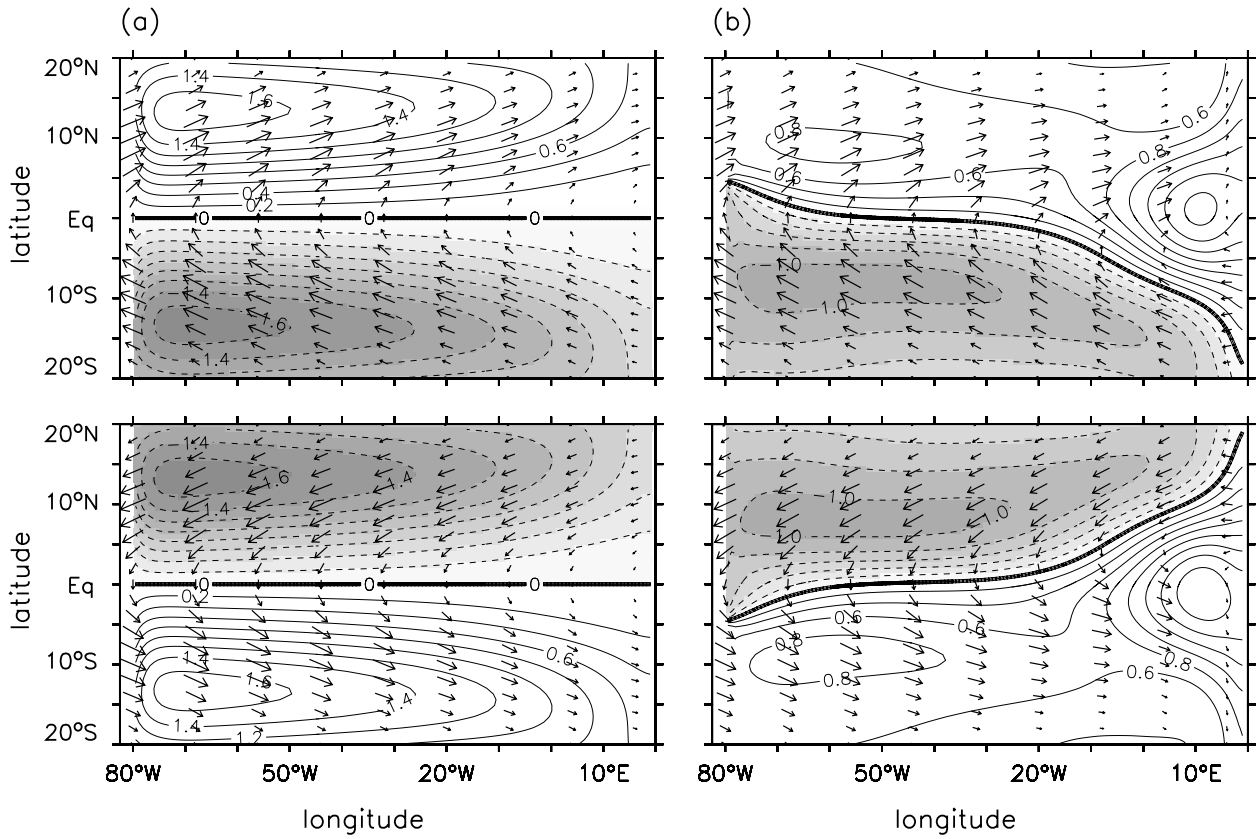

Figure 2

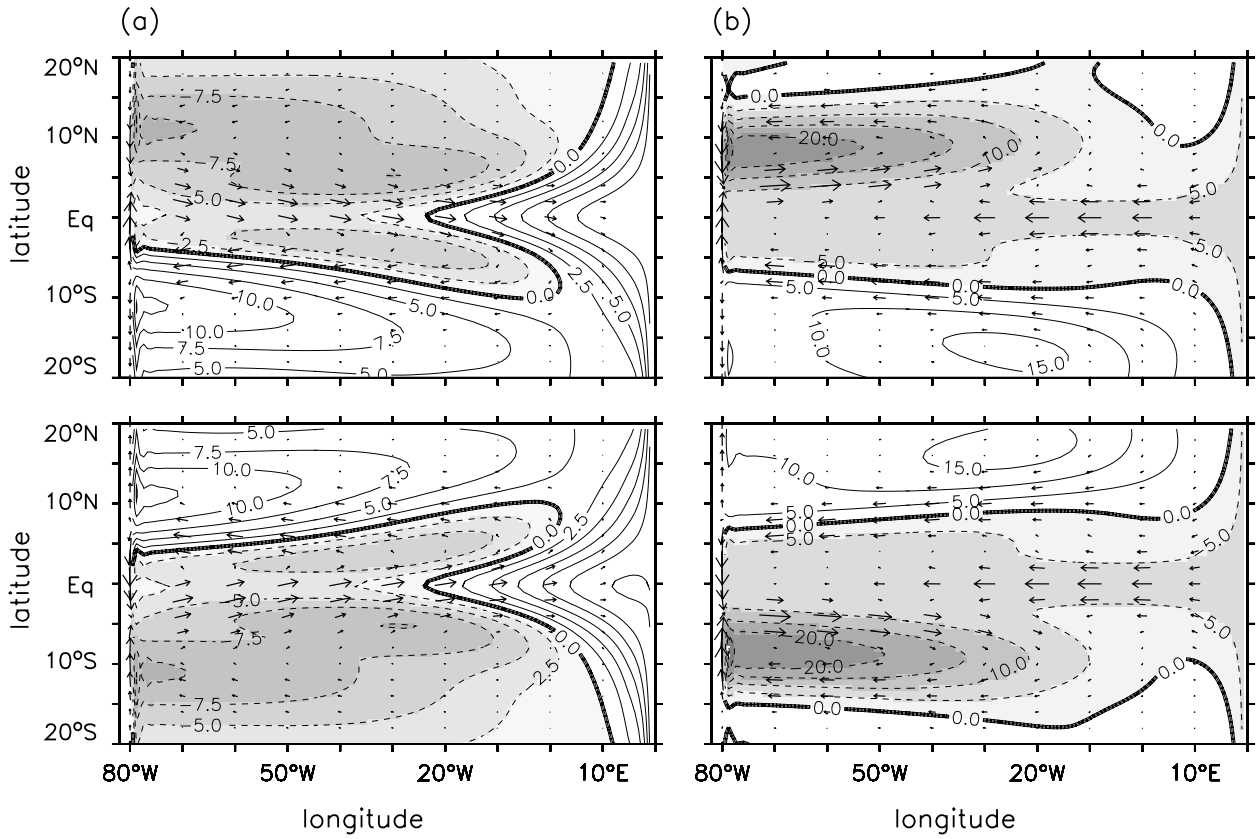

Figure 3

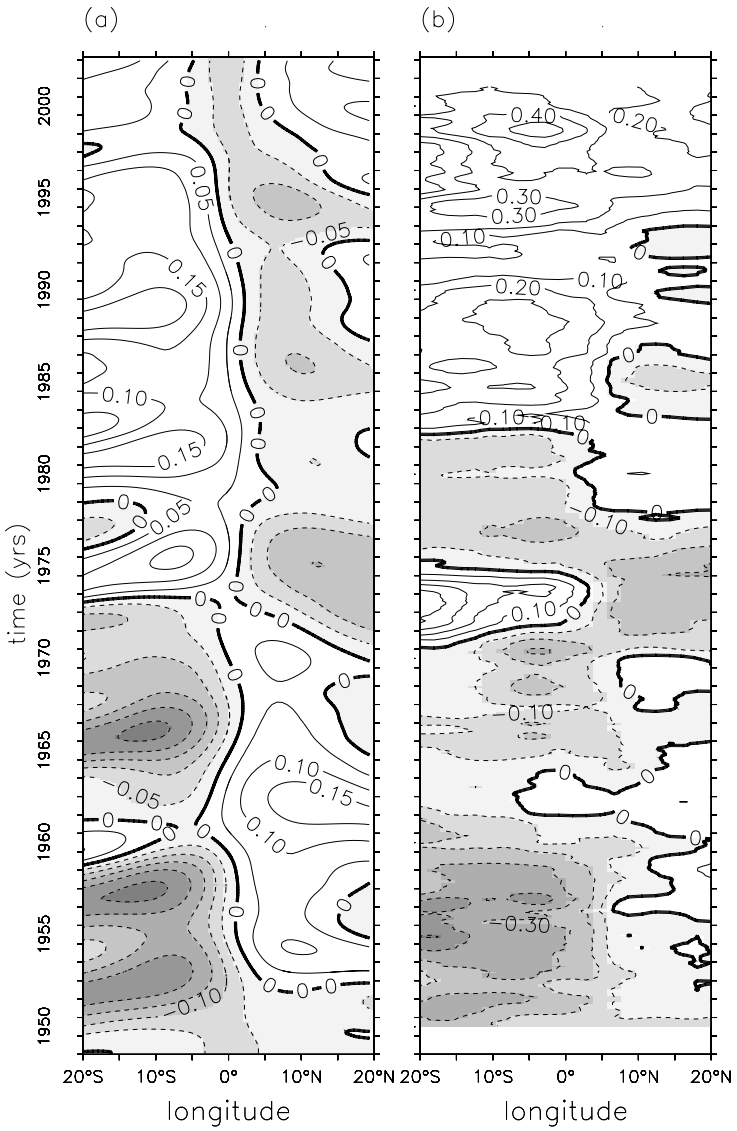
(a)
(b)
time (yrs)
1950
1955
1960
1965
1970
1975
1980
1985
1990
1995
2000
20°S
10°S
0°
10°N
20°N
longitude
longitude

Figure 4

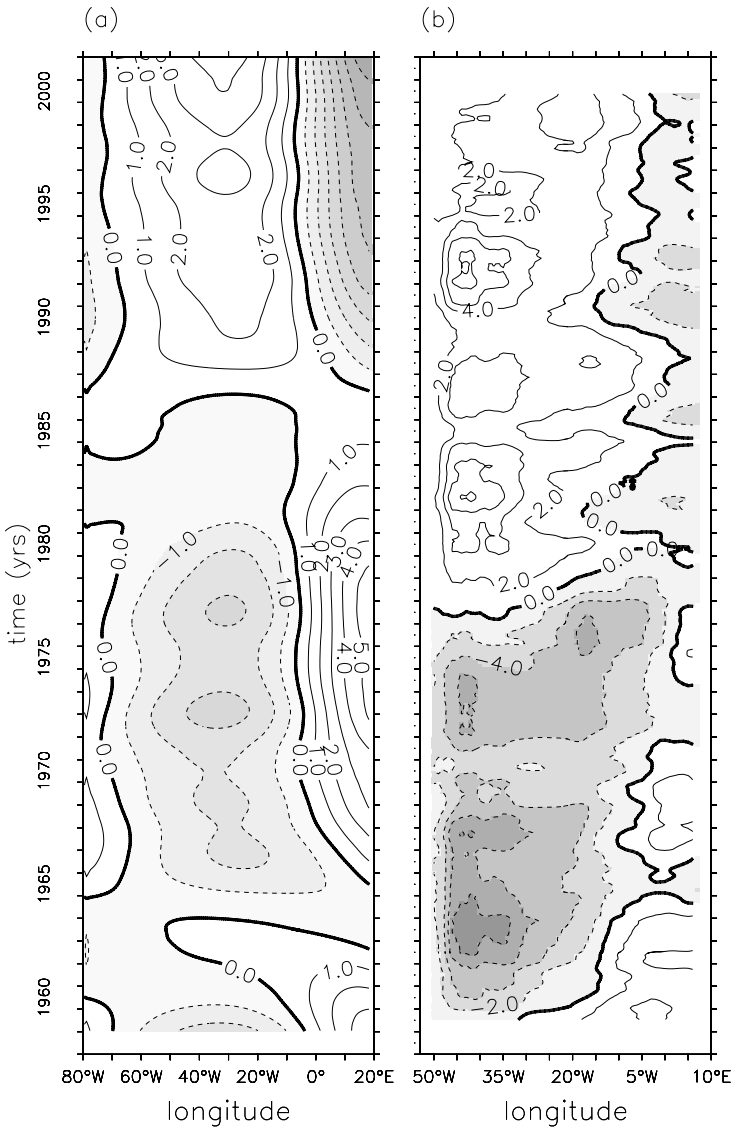
(a)
(b)
time (yrs)
2000
1995
1990
1985
1980
1975
1970
1965
1960
80°W
60°W
40°W
20°W
0°
20°E
50°W
35°W
20°W
5°W
10°E
longitude
longitude

Figure 5

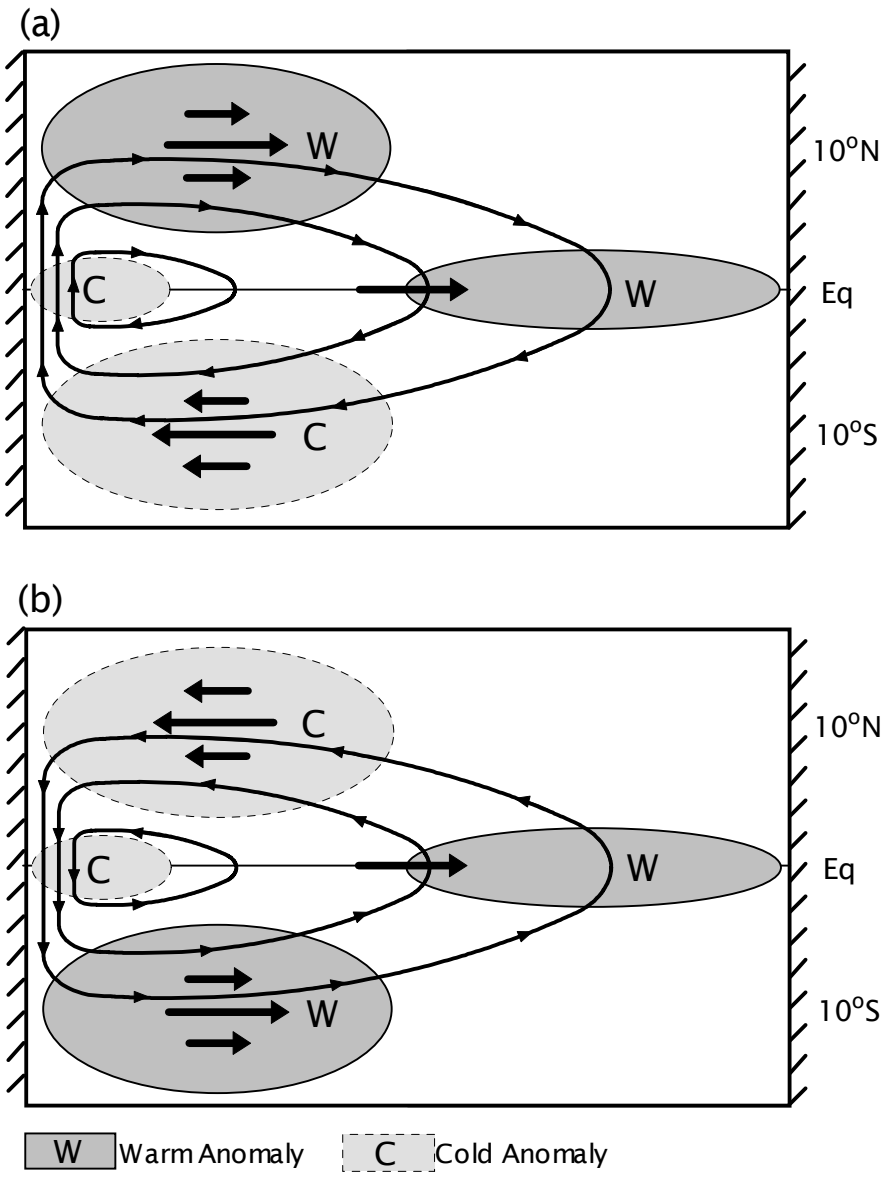
(a)
W
C
W
C
10°N
Eq
10°S
(b)
C
C
W
W
10°N
Eq
10°S
W Warm Anomaly
C Cold Anomaly

Figure 6